arXiv:1111.4365v1 [cond-mat.mes-hall] 18 Nov 2011

Effect of a gap on the decoherence of a qubit

Juliana Restrepo[1], R. Chitra[1], S. Camalet[1] and Émilie Dupont[2].
[1] *Laboratoire de Physique Théorique de la Matière Condensée, UMR 7600,*
Université Pierre et Marie Curie, 4 place Jussieu, 75252 Paris Cedex 05, France.
[2] *Laboratoire de Physique Théorique et Modélisation, CNRS UMR 8089,*
Université de Cergy-Pontoise, F-95000 Cergy-Pontoise, France
(Dated: November 21, 2011)

We revisit the problem of the decoherence and relaxation of a central spin coupled to a bath of conduction electrons. We consider both metallic and semiconducting baths to study the effect of a gap in the bath density of states (DOS) on the time evolution of the density matrix of the central spin. We use two weak coupling approximation schemes to study the decoherence. At low temperatures, though the temperature dependence of the decoherence rate in the case of a metallic bath is the same irrespective of the details of the bath, the same is not true for the semiconducting bath. We also calculate the relaxation and decoherence rates as a function of external magnetic fields applied both on the central spin and the bath. We find that in the presence of the gap, there exists a certain regime of fields, for which surprisingly, the metallic bath has lower rates of relaxation and decoherence than the semiconducting bath.

PACS numbers: 03.65Yz, 76.20+q, 71.20Nr

I. INTRODUCTION

Solid state spin devices are promising candidates for quantum computation[1] and for quantum communication[2]. The basic building block for quantum computation is the qubit, which is an effective two level system. Various realizations of qubits include spins, Josephson junction qubits[3] and others involving quantum dots[4]. The efficiency of these systems as qubits/quantum computing devices depends crucially on their coupling to the numerous environmental degrees of freedom. Typically, environments are composed of phonons, electrons, nuclear spins or other noise inducing objects and lead to dissipation and a consequent loss of coherence of the qubit. Understanding the dependence of this decoherence and relaxation on the physical parameters which define the environment is vital to fabricating good qubits.

The simplest models used to study the effects of dissipation induced by the environment is the Caldeira-Leggett model[5], and the spin-boson[6] model where a central spin couples to a bath of free bosons. The past decade has however, seen a lot of studies on various kinds of dissipative environments including interacting and non-interacting spin baths and electronic baths[7–12]. In the limit of weak coupling between the central spin i.e., qubit and the bath, intra-bath interactions were sometimes seen to have a mitigating effect on the decoherence but this is not generically true[7]. The effect of fermionic environments on single and multiple qubit systems has also been studied in[9,13–15]. The ensuing decoherence also depends on the nature of the coupling between the qubit and the bath fermions. In general, one expects Markovian decay of the coherence of the qubit at finite temperatures. However, unlike the case of bosonic baths, where the decoherence rate increases indefinitely with temperature, the rate saturates with temperature for spin and fermionic baths. This is however, not the case if there is long range order present in the bath or when the bath exhibits glassy features[8,16].

In this paper, we revisit the problem of decoherence induced by a simple fermionic environment weakly coupled to a qubit i.e., a central spin. We consider a Kondo coupling where the central spin interacts with the local spin density of the bath fermions at the central spin site and focus on the effect of different metallic and insulating densities of states, in particular, that of a direct gap in the density of states. In the weak coupling limit, we use the well known time-convolutionless (TCL) and Nakajima-Zwanzig (NZ) techniques[17] to study decoherence. Though the two methods are equivalent for metallic density of states (DOS), we see that these two approximations are inequivalent for a semi-conducting DOS at low enough temperatures raising questions about the validity of the weak coupling approximations in certain limits[18]. We find that in general the asymptotic decoherence is qualitatively the same for a bath with a metallic DOS, though details of the DOS are very relevant for determining the intermediate time behavior. Furthermore, we also calculate the relaxation and decoherence rates, γ_1 and γ_2 as a function of external magnetic fields applied both on the environment and the central spin.Though the metallic or semiconducting nature of the bath plays an important role at low temperatures, the baths are qualitatively indistinguishable at higher temperatures.

The paper is organized as follows: in Sec. II, we introduce the model and the weak coupling formalism used to obtain the decoherence and relaxation of the central spin. We investigate the case of zero magnetic fields in Sec. III. Our results for the coherence of a qubit coupled to a metallic and a semiconducting bath at zero and finite temperatures are presented in Sec. III A and Sec. III B. In Sec. IV, we study the dependence of both the relaxation and decoherence rates on external magnetic fields applied on the qubit and bath respectively followed by a

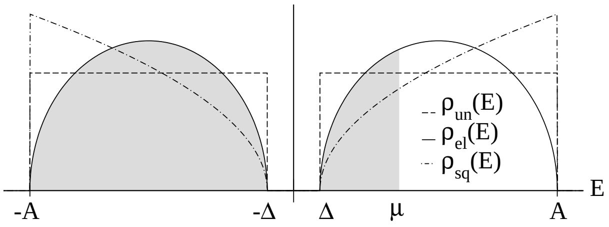

FIG. 1. Densities of states $\rho_{un}(E)$ (dashed lines), $\rho_{el}(E)$ (bold lines), $\rho_{sq}(E)$ (dot-dashed lines) as a function of E for a metal $\mu > \Delta$.

brief discussion of our results in Sec. V.

II. WEAK COUPLING FORMALISM

We present the model Hamiltonian and the methodology used to study the reduced dynamics of the central spin interacting with a bath. The Hamiltonian that describes a localized spin-$\frac{1}{2}$ $\boldsymbol{\sigma}_c$ coupled to a bath of non-interacting electrons is given by:

$$\begin{aligned} H =& H_S + H_B + H_{SB} \\ H =& -h\sigma_c^z + \sum_{k\alpha} \varepsilon_{k\alpha} c_{k\alpha}^\dagger c_{k\alpha} - \boldsymbol{\sigma}_c.\mathbf{V} \end{aligned} \tag{1}$$

where H_S denotes the intrinsic Hamiltonian of the central spin described by the Pauli matrices $\boldsymbol{\sigma}_c$ subjected to a magnetic field h, H_B denotes the bath of non-interacting electrons and H_{SB} describes the Kondo coupling between the central spin and the bath with $\mathbf{V} = \lambda \sum_{k,p,\alpha,\beta} c_{k\alpha}^\dagger \boldsymbol{\sigma}_{\alpha\beta} c_{p\beta}$ proportional to the spin density of the bath electrons at the origin where the central spin is positioned. The coupling constant λ is smaller than all the other scales of the hamiltonian. $c_{k\alpha}$,$c_{k\alpha}^\dagger$ are the fermionic annihilation and creation operators with wave number k and $\varepsilon_{k\alpha} = \varepsilon_k + \alpha H$ ($\alpha = \pm 1$) denotes the dispersion of the two spin species of the bath electrons subjected to an external magnetic field H.

To study the evolution (decoherence and relaxation) of the central spin, we assume that at time $t = 0$, the central spin is in a pure state $|\psi\rangle = \alpha|\uparrow\rangle + \beta|\downarrow\rangle$ and that the bath is in thermal equilibrium at temperature T. This leads to a factorizable initial density matrix $\Omega = \rho_s(0) \otimes \rho_B$ where $\rho_s(0) = |\psi\rangle\langle\psi|$ and

$$\rho_B = \frac{e^{-H_B/T}}{Z} \tag{2}$$

where $Z = \mathrm{Tr}\left[\exp\left(-\beta H_B\right)\right]$ is the bath partition function. We use units $\hbar = k_B = 1$ throughout this paper. The time evolution of the reduced density matrix of the central spin is given by

$$\rho_s(t) = \mathrm{Tr}_B\left[e^{-iHt}\Omega e^{iHt}\right] \tag{3}$$

where Tr_B is the partial trace over the bath degrees of freedom. We rewrite the density matrix (3) as a Laplace transform

$$\begin{aligned} \rho_s(t) \equiv& \frac{i}{2\pi}\int_{R+i\eta} dz e^{-izt} \rho_s(z) \\ =& \frac{i}{2\pi}\int_{R+i\eta} dz e^{-izt} \mathrm{Tr}_B\left[(z-\mathcal{L})^{-1}\rho(0)\otimes\rho_B\right] \end{aligned} \tag{4}$$

where η is a real positive number and $\mathcal{L}$ is the Liouville operator corresponding to the total Hamiltonian H, i.e., $\mathcal{L}A = [H, A]$ for any operator A. The density matrix can be decomposed in the basis of Pauli spin operators as follows:

$$\rho_s(z) = \frac{1}{2}\sum_{\alpha=0,x,y,z} M_\alpha(z)\sigma_c^\alpha \tag{5}$$

The decoherence and relaxation are given by the quantities M_α which are in general rather difficult to calculate. However, for weak central spin-bath coupling i.e., $\lambda \to 0$, we can use perturbation theory in conjunction with the projection operator technique to calculate the components M_α[19]. These lead to equations for M_α which go beyond the standard Markovian master equation. To second order in λ, the $M_\alpha(z)$ satisfy the following matrix equation

$$zM_\beta(z) - \sum_\alpha h_{\beta\alpha} M_\alpha(z) - \sum_\alpha \Sigma_{\beta\alpha}(z) M_\alpha(z) = \langle\sigma_c^\beta\rangle_0 \tag{6}$$

where $\Sigma_{\alpha\beta}$ are the self-energies and only $h_{xy} = h_{yx}^* = 2ih$ are nonzero. In the absence of external magnetic fields ($h = H = 0$), since we have a SU(2) invariant bath (i.e., $\varepsilon_{k\alpha} = \varepsilon_{k-\alpha}$), the self energy matrix simplifies with the only non-zero entries being the diagonal terms $\Sigma_{xx} = \Sigma_{yy} = \Sigma_{zz} \equiv \Sigma$. These diagonal self-energies are related to the bath correlation function

$$\Sigma(z) = -8i\int_0^\infty dt e^{izt}\left[\Re e\langle\tilde{V}_x(t)\tilde{V}_x\rangle\right] . \tag{7}$$

where for any operator A, $\tilde{A}$ is defined as $\tilde{A}(t) = e^{iH_Bt}Ae^{-iH_Bt} - \langle A\rangle$ and $\langle\ldots\rangle$ denotes the thermal expectation value, i.e.,$\langle A\rangle = \mathrm{Tr}(A\rho_B)$ for any operator A. Consequently, $M_x = M_y = M_z \equiv M$ with M being given by

$$M(z) = \frac{1}{z - \Sigma(z)} \tag{8}$$

The exact expressions of $h_{\alpha\beta}$ and $\Sigma_{\alpha\beta}$ for the general case are detailed in the appendix.

To obtain $M(t)$ and hence $\rho_s(t)$, we first analytically continue Σ to real frequencies ω

$$\lim_{\eta\to 0^+} \Sigma(\omega + i\eta) = \Lambda(\omega) - i\Gamma(\omega) \tag{9}$$

where Λ and Γ are related by the Kramers-Kronig relation.

$$\Lambda = -\frac{1}{\pi}P\int \frac{\Gamma(\omega')}{\omega' - \omega} d\omega \tag{10}$$

Note that Γ is even in ω whereas Λ is odd. For the case of the electronic bath studied here, calculating the correlation in Eq.(7), we find that Γ is given by

$$\Gamma(\omega) = 8\pi\lambda^2 \left[S(\omega) + S(-\omega)\right] \tag{11}$$

where $S(\omega)$ is the dynamical spin structure factor for the bath and given by

$$S(\omega) = \int dE\rho(E)\rho(E+\omega)n(E)\left[1 - n(E+\omega)\right] \tag{12}$$

In Eq.(12), $\rho(E)$ is the density of states (DOS) for the bath and $n(E)$ is the Fermi occupation number.

The inverse Laplace transform of $M(z)$ directly gives the Nakajima-Zwanzig (NZ) approximation for the coherence

$$M_{NZ}(t) = \frac{1}{\pi}\int_0^{\infty} d\omega \cos(\omega t)\tilde{\Gamma}(\omega) \tag{13}$$

where

$$\tilde{\Gamma}(\omega) = \Gamma(\omega)/\left[(\omega - \Lambda(\omega))^2 + \Gamma(\omega)^2\right] \tag{14}$$

On the other hand, if the self energy $\Sigma(z)$ is analytic in the lower half plane[8], we obtain a simplified form for the coherence which is the well known time convolutionless approximation (TCL)

$$\ln M_{TCL}(t) \simeq -\frac{2}{\pi}\int_{-\infty}^{\infty} d\omega \frac{\sin(\omega t/2)^2}{\omega^2}\Gamma(\omega) \tag{15}$$

Note that the NZ approximation corresponds to a master equation which is non-local in time i.e., it has a memory kernel, whereas TCL approximation corresponds to a purely local in time master equation[20]. Though the TCL is local in time, the time-integration over the memory kernel is the characteristic feature which can capture the non-Markovian nature of the dynamics. If $\Sigma(z)$ is analytic in the lower half plane, both techniques lead to the same asymptotic behavior for the coherence but they might yield different results in cases where $\Sigma(z)$ is not analytic. As we shall show later, the two methods converge for the case of metallic DOS wherein Σ is analytic in the lower half plane, but they predict different results for the simple case of a semiconducting DOS, because of the presence of weak non-analyticities on the real axis.

In the presence of external magnetic fields, the self-energy matrix $\Sigma_{\beta\alpha}$ has a far more complicated structure than the one described above and requires a full matrix inversion to obtain the coherences M_α. However, the two timescales T_1 (rate γ_1) and T_2 (rate γ_2) which determine the asymptotic relaxation and decoherence i.e., $\langle\uparrow|\rho_S(t)|\uparrow\rangle \sim \exp\left[-t/T_1\right]$ and $\langle\uparrow|\rho_S(t)|\downarrow\rangle \sim \exp\left[-t/T_2\right]$ are given by the bath correlation functions as[21]:

$$\gamma_1 = \frac{1}{T_1} = \int dt e^{2iht}\left[\langle\tilde{V}_+(t)\tilde{V}_-\rangle + \langle\tilde{V}_-\tilde{V}_+(t)\rangle\right] \tag{16}$$

$$\gamma_2 = \frac{1}{T_2} = \frac{1}{2T_1} + 2\int dt\Re e\langle\tilde{V}_z(t)\tilde{V}_z\rangle \tag{17}$$

with $\tilde{V}_\pm = \tilde{V}_x \pm i\tilde{V}_y$.In the rest of the paper, we use the dimensionless rates $\bar{\gamma}_{1,2} = \gamma_{1,2}/8\pi\lambda^2$. Note that for $h = H = 0$, we have $\bar{\gamma}_1 = \bar{\gamma}_2 = \bar{\gamma}$.

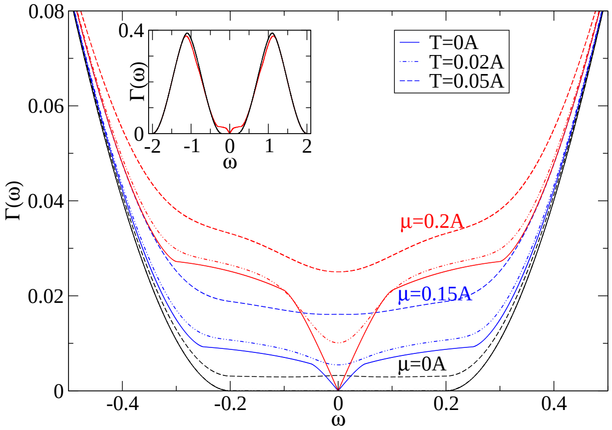

FIG. 2. (color online) Low frequency behavior of $\Gamma(\omega)/8\pi\lambda^2 N^2$ as a function of ω (units of A) for different values of the chemical potential: $\mu = 0$ (black), $\mu = 0.15A$ (blue), $\mu = 0.2A$ (red) and temperature: $T = 0$ (bold lines), $T = 0.02A$ (dot-dashed lines), $T = 0.05A$ (dashed lines) for the elliptical density with $\Delta = 0.1A$. In the Figure, the temperatures $T = 0$, $T = 0.02A$ are indistinguishable for $\mu = 0A$. The inset shows the full $\Gamma(\omega)/8\pi\lambda^2 N^2$ for a metal at $\mu = 0.2A$ (red) and a semiconductor $\mu = 0$ (black) at zero temperature.

III. ZERO MAGNETIC FIELD

We now use the weak coupling formalism presented in the previous section to calculate the coherence $M(t)$ for fermionic baths having both metallic and insulating density of states. In order to study the effect of the details of the DOS on the asymptotic coherence, we consider three densities of states: uniform, square root and elliptical, each of which has a gap Δ and a cut-off A:

$$\begin{aligned}
\rho_{un}(E) &= \frac{1}{2(A-\Delta)}\Theta(|E|-\Delta)\Theta(A-|E|) \\
\rho_{sq}(E) &= N\sqrt{|E|-\Delta}\,\Theta(|E|-\Delta)\Theta(A-|E|) \\
\rho_{el}(E) &= N'\left(\frac{(A-\Delta)^2}{4} - \left(|E| - \frac{(A+\Delta)}{2}\right)^2\right)^{\frac{1}{2}}
\end{aligned} \tag{18}$$

where the normalization constants $N = \frac{3}{4}(A-\Delta)^{-\frac{3}{2}}$ and $N' = \frac{16}{3\pi}N(A-\Delta)^{-\frac{1}{2}}$ have been chosen so that all densities of states have the same normalization. Depending on the chemical potential μ, one obtains a metallic bath for $\mu > \Delta$ and a semiconducting bath for $\mu < \Delta$. Though real semiconductors have more complicated DOS, we nonetheless expect the simple DOS used in this paper to capture the essential features of the asymptotic relaxation and decoherence induced by such baths. The gaps in semiconductors are typically of the order of 1 eV: 1.12 eV for Silicon and 0.66 eV for Germanium[22] and the cut-off A is of the order of 10 eV.

A. Metallic bath

Here we assume that the chemical potential $\mu > \Delta$. At zero temperature and for small frequencies ω, using Eqs. (11) and (12), we obtain the generic result $\Gamma(\omega) = 2K|\omega|$ reminiscent of the Ohmic behavior seen in the standard spin-boson problem[6]. The coefficient K depends on the DOS and we find that $K_{un} = \pi\lambda^2/(A-\Delta)^2$, $K_{sq} = 4\pi\lambda^2 N^2(\mu-\Delta)$ and $K_{el} = 4\pi\lambda^2 N^2 \left(\frac{16}{3\pi}\right)^2 (A-\Delta)^{-1}(\mu-\Delta)(A-\mu)$. The fact that K_{un} is independent of μ is an artifact of the uniform DOS. This Ohmic bath leads to the expected power law decay of the decoherence $M(t) \simeq t^{-4K/\pi}$ where for the different DOS, the appropriate value of K should be substituted. The asymptotic decoherence induced by a metallic bath is qualitatively similar to that induced by a bosonic bath at $T = 0$. This correspondence with the spin-boson problem does not hold true at finite temperatures or in the presence of magnetic fields as we will show later. The full behavior of $\Gamma(\omega)$ for the case of the elliptical DOS is plotted in Fig 2 for various temperatures and chemical potentials.

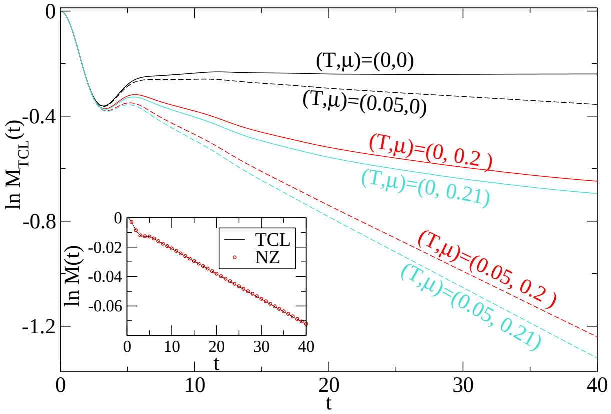

FIG. 3. (color online) $\ln M_{TLC}/8\pi\lambda^2 N^2$ as a function of t for a $\mu = 0$ (black), 0.2 (red), 0.21 (turquoise) and $T = 0$ (bold-lines), 0.05 (dashed-lines) for the elliptical DOS with $\Delta = 0.1$. In the inset, we plot $\ln M/N^2$ for NZ and TCL approximations for $(T,\mu) = (0.1, 0.2)$ and $\lambda = 0.05$. Time, gap, chemical potential and coupling strength are in units of A.

At finite temperature, we see two principal features: $\Gamma(\omega = 0) \neq 0$ and $\Gamma(\omega)$ is fully analytic. These features are also seen for the square root DOS but one encounters non-analyticities for the uniform DOS because of the discontinuities in the band structure. However, Γ is expected to be analytic for realistic metallic DOS. For a given band filling, the low frequency behavior of Γ is found to be qualitatively the same for both square root and elliptical density of states, implying that the asymptotic behavior is indeed similar in both cases. For $T \neq 0$, both approximations TCL and NZ predict a Markovian decay of the coherence for times $t \gg t_T \sim 1/T$, with a decay rate $\gamma = \Gamma(0)$ as shown in Fig. 3. The equivalence of TCL and NZ at all times is clearly illustrated in the inset of Fig. 3. For a metallic DOS, the decoherence rate $\bar{\gamma} \propto T$ at low T and $\bar{\gamma} \propto T \tanh A/T$ as $T \to \infty$ where A is the cut-off. For $\rho_{un}(E)$ at low temperatures the exact result is $\bar{\gamma} = 2T(2 - e^{-(\mu-\Delta)/T})$. Note that the temperature independent proportionality factors are dependent on the details of the bath DOS. In Fig. 4, we plot the rate $\bar{\gamma}$ for metallic bath $\mu > \Delta$ for both square root and elliptical DOS. As seen in the case of interacting spin baths[8], $\bar{\gamma}$ increases with temperature and saturates to a finite DOS-dependent value proportional to $\int \rho(E)^2 dE$ at high temperatures. This saturation stems from the fact that the electrons have a spin degree of freedom and is different from the case of a bosonic bath, where the decoherence rate never saturates. Fig.3 also shows that a higher chemical potential results in a faster decoherence at all temperatures as there are more carriers which can dissipate energy. To summarize, in the weak coupling limit, both second order TCL and NZ schemes predict that a simple metallic bath results in a power law decay of the asymptotic coherence at $T = 0$ and a Markovian decay at $T \neq 0$ irrespective of the nature of the underlying DOS. The corresponding exponents and the Markovian rate do not depend very much on the qualitative details of the DOS. However, we expect the intermediate and other short time regimes to be indeed dependent on the details of the DOS.

To understand whether the presence of a gap in the DOS below the Fermi energy has any impact whatsoever on the decoherence, we plot Γ in the right panel of Fig. 5 for the elliptic DOS for $\Delta = 0$ and $\Delta \neq 0$ at the same value of the filling. At $T = 0$, though the low frequency behavior is the same in both cases, a plateau like structure is indeed seen in the vicinity of $\omega \sim 2\Delta$ when $\Delta \neq 0$. We observe that for asymptotic times,

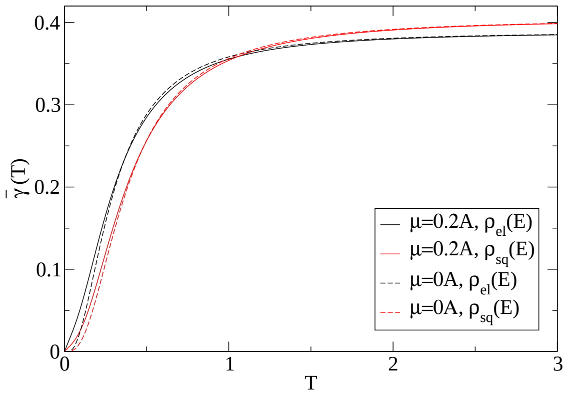

FIG. 4. (color online) Dimensionless rate $\bar{\gamma}/N^2$ as a function of temperature in units of A for a semiconductor $\mu = 0$ (dashed lines) and a metal $\mu = 0.2A$ (bold lines) for the elliptical (black) and square root (red) DOS with $\Delta = 0.1A$.

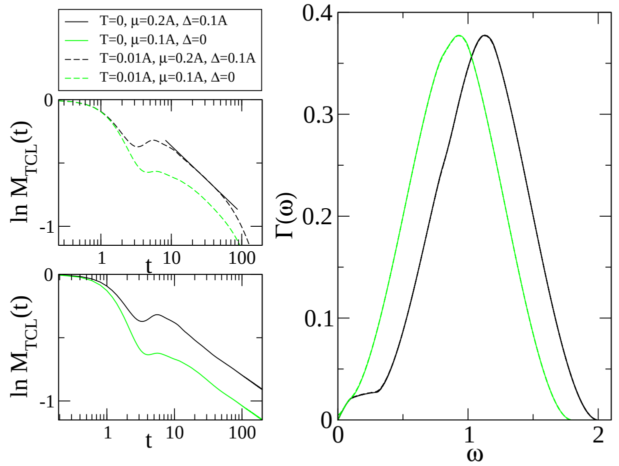

FIG. 5. Left panel: $\ln M_{TLC}/8\pi\lambda^2 N^2$ as a function of t for $\Delta = 0$ (green) and $\Delta = 0.1A$ (black) at $T = 0$ (bold lines) and $T = 0.01A$ (dashed lines). Right panel: Full $\Gamma(\omega)/8\pi\lambda^2 N^2$ as a function of ω for $\Delta = 0$ and $\Delta = 0.1A$ at $T = 0$.

$M(t) \propto Ct^{-\kappa}$ where C is some constant which depends on the bath parameters and λ. We find that though the exponent κ is the same irrespective of the value of Δ, the coefficient C is indeed dependent on Δ resulting in a faster decoherence in the gapless case cf. top left panel of Fig. 5. At low temperatures, as seen in the bottom left panel of Fig. 5, though both DOS have an asymptotic Markovian regime with the same decay rate, the DOS with a gap has an intermediate power law regime for times $t_\Delta \sim 1/\Delta < t \ll t_T$ which is not present for the gapless metallic bath because $t_\Delta \sim \infty$. This intermediate regime can be quite large depending on the parameters of the problem. To summarize, a gap in the DOS below the Fermi energy does serve to reduce decoherence as compared to the case of a gapless DOS and this feature could probably be exploited in experiments.

B. Semiconductor bath

We now focus on the semiconductor bath with a gap at the fermi level. At zero temperature, $\Gamma(\omega) = 0$ for $\omega \leq 2\Delta$ and $\Gamma(\omega) \propto \lambda^2(\omega - 2\Delta)^2$ for ω close to 2Δ for all DOS. The full behavior of $\Gamma(\omega)$ for the elliptical DOS is plotted in Fig. 2. We first focus on the TCL results. At $T = 0$, we find that due to the presence of a gap in Γ, the central spin only decoheres partially. A straightforward evaluation of (15) shows the existence of three regimes: a short time regime $t_A \ll 1/A$ where the central spin initially decoheres as a Gaussian followed by an oscillatory regime for $t < t_\Delta$ with a well defined minimum around $\bar{t} \simeq 4/(2\Delta + A)$ and the asymptotic regime for $t > t_\Delta$, where $M(t) \to \mathit{const}$ as a power law. These three regimes are expected to be generic and are indeed seen in the full numerical results for the coherence for both square root and elliptical DOS (see Fig. 3).

As temperature increases, the thermal activation of the gap results in a Γ which is no longer gapped (cf. Fig. 2). Within the TCL formalism, this immediately implies that the asymptotic behavior is Markovian $\ln M_{TCL}(t) \simeq -\gamma t$. For low enough temperatures $T \ll \Delta$ which is the real semiconducting regime, we have the usual Gaussian behavior for $t < t_A$, followed by an oscillatory regime for $t_A \ll t \ll t_\Delta$, a power-law intermediate regime for $t_\Delta \ll t \ll t_T$ and finally the asymptotic Markovian regime for $t > t_T$ (cf. Fig. 3). At high temperatures $T \gg \Delta$, there is no difference between the metal and the semiconductor and the intermediate power law regime ceases to exist.

In contrast to the metallic case, where the decoherence rate seemed to have the same qualitative behavior for all the DOS considered, the rate in the semiconducting case seems to be DOS dependent as $T \to 0$. In this limit, $\bar{\gamma} \propto T^2 \exp -(\Delta - \mu)/T$ for $\rho_{sq}(E)$ and $\rho_{el}(E)$ and $\bar{\gamma} \propto T \exp -(\Delta - \mu)/T$ for $\rho_{un}(E)$. Comparing with the case of the metallic bath where $\bar{\gamma} \propto T$, we see that the semiconducting bath has a much smaller rate and hence longer coherence times which makes it a better environment for qubits than a simple metal. However, as T increases, $\bar{\gamma}$ has the same qualitative behavior as indicated in Fig. 4. At higher temperatures, since the gap is completely smeared by thermal effects as expected there is no real difference between the metallic and the semiconducting baths.

We now address the question of whether NZ predicts similar results for the asymptotic decoherence in the semiconducting case. Substituting $\Lambda(\omega)$ obtained from Eq. (10) in (14), we find that $\widetilde{\Gamma}(\omega)$ typically has a three peak structure. At low temperatures, $\widetilde{\Gamma}(\omega)$ can be rewritten as the sum of two disjoint contributions $\widetilde{\Gamma}(\omega) = \widetilde{\Gamma}^l(\omega) + \widetilde{\Gamma}^s(\omega)$ where $\widetilde{\Gamma}^l$ is a Lorentzian peak at low frequencies and $\widetilde{\Gamma}^s$ describes two small satellite peaks which exist for $\omega \geq 2\Delta$. This separation of spectral weight in $\widetilde{\Gamma}$ leads to $M_{NZ}(t) = M^l_{NZ}(t) + M^s_{NZ}(t)$ where the first term is the usual Markovian decay $M^l_{NZ}(t) \simeq \exp -\gamma t$ with γ being the same as that given by the TCL approximation. To estimate the correction $M^s_{NZ}(t)$ stemming from the satellite peaks, we note that for $\omega \gtrsim 2\Delta$, $\Lambda(\varepsilon) \simeq \Lambda_0 + \varepsilon\Lambda_1 + \varepsilon^2\Lambda_2 + \varepsilon^2 \ln \varepsilon + O(\varepsilon^3)$ where $\varepsilon = \omega - 2\Delta$. Consequently,

$$\widetilde{\Gamma}^s(\omega) \simeq \frac{\pi^2\lambda^2}{(\Lambda_0 - 2\Delta)^2}(\omega - 2\Delta)^2 \qquad (19)$$

Using (19) and (13), we find that for long times

$$M^s_{NZ}(t)/\pi\lambda^2 \sim \frac{1}{4\Delta^2}(E_c - 2\Delta)^2 \sin{(E_c t)}/t \qquad (20)$$

where $E_c \gtrsim 2\Delta$ is a cut-off scale for which $\widetilde{\Gamma}^s(\omega)$ has a quadratic behavior. The true asymptotic behavior predicted by the NZ scheme now depends on the competition between the exponential and the power law terms. This defines a new time scale $t_{nz} \propto 1/\gamma \log(1/B\gamma)$ where B is the pre-factor of the power law term seen in Eq.(20) such that for $t_T < t < t_{nz}$ one obtains the usual Markovian behavior, whereas for $t \gg t_{nz}$ one sees a non- Markovian power law decay of the coherence. In the weak coupling formalism used here, λ is expected to be much smaller than all the other scales of the hamiltonian, so a t_{nz} of the order of λ^{-2} does correspond to very very long times for which the coherence has already decayed to infinitesimal values and is practically unobservable. A full numerical integration of (13) with the appropriate $\widetilde{\Gamma}$ does show the existence of these two asymptotic regimes $M^s_{NZ}(t)$ and $M^l_{NZ}(t)$ at low temperatures. For higher temperatures, the gap in $\widetilde{\Gamma}$ is completely smeared by thermal fluctuations and one recovers the pure Markovian decay. The preceding analysis shows that the two approximations TCL and NZ do not necessarily predict same results in the weak coupling limit even for simple environments like the semiconductor considered in this section. This divergence between the TCL and NZ approximations has been seen in other problems like spin baths where exact solutions are known[20]. This shows that one should exercise caution when using these approximation schemes to calculate coherences in the cases of baths with more complicated characteristics.

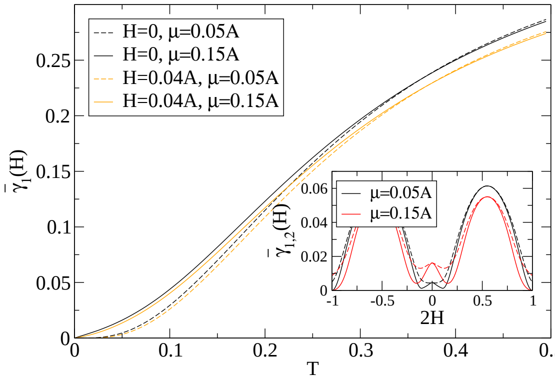

FIG. 6. (color online) Dimensionless relaxation rate $\bar{\gamma}_1(H)/N^2$ as a function of temperature in units of A for a semiconductor $\mu = 0.05A$ (dashed lines) and a metal $\mu = 0.15A$ (bold lines) for fields $H = 0$ (black) and $H = 0.04A$ (orange) for the elliptical DOS with $\Delta = 0.1A$. Inset: Dimensionless decoherence (dashed lines) and relaxation (bold lines) rates $\bar{\gamma}_{1,2}(H)/N^2$ as a function of $2H$ for a semiconductor $\mu = 0.05A$ (red) and a metal $\mu = 0.15A$ (black) at $T = 0.05A$.

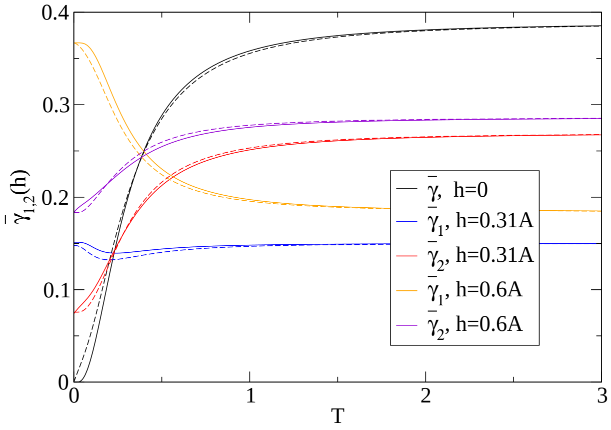

FIG. 7. Dimensionless decoherence and relaxation rates $\bar{\gamma}_{1,2}(h)/N^2$ for a semiconductor $\mu = 0$ (dashed lines) and a metal $\mu = 0.2A$ (bold lines) as a function of temperature for different values of h, $H = 0$ and an elliptical DOS with $\Delta = 0.1A$. Temperature is in units of A.

IV. NON-ZERO MAGNETIC FIELD

In this section, we study the dependence of the asymptotic decoherence and relaxation rates on magnetic fields H and h applied on the bath electrons and the central spin respectively cf. Eq.1. We explore whether an interplay between the magnetic fields can be used as a way to control decoherence and relaxation. Calculating the in-plane correlation functions $\langle \tilde{V}_{x,y}(t)\tilde{V}_{x,y}\rangle$ and the perpendicular correlation function $\langle \tilde{V}_z(t)\tilde{V}_z\rangle$ and using them in Eqs. (16) and (17), the dimensionless decoherence and relaxation rates are given by:

$$\bar{\gamma}_1 = \sum_{p=\pm 1}\int dE\rho(E)\rho(E+2p(H+h)) \qquad (21)$$

$$\times\, n(E+pH)\left[1-n(E+p(2h+H))\right]$$

$$\bar{\gamma}_2 = \frac{1}{2}\bar{\gamma}_1 + \frac{1}{2}\sum_{p=\pm 1}\int \rho(E)^2 n(E+pH)\left[1-n(E+pH)\right] \qquad (22)$$

In the following, we assume $h, H \geq 0$. We clearly see that for $H = h = 0$, $\bar{\gamma}_1 = \bar{\gamma}_2$. For the special case of the Ising coupling $\mathbf{V} = (V_x, 0, 0)$ we have $\bar{\gamma}_2 = \bar{\gamma}_1/2$ for all fields. As we shall see below, we have a rich spectrum of behavior for the two rates as a function of field for all DOS. Though the plots Fig.6-8 show the numerical results for the elliptical density $\rho_{el}(E)$ only, we find that the key qualitative features summarized below are true for all the DOS considered in this paper. The qualitative features of these results are seen for all the other DOS as well. Additionally, we focus on low and intermediate temperatures, since the metallic ($\mu > \Delta$) and semiconducting ($\mu < \Delta$) baths are indistinguishable at high temperatures.

A. $h = 0, H \neq 0$

Our results for the two rates $\bar{\gamma}_1$ and $\bar{\gamma}_2$ as a function of H and T are plotted in Figs. 6-8 for both metallic and semiconducting baths. We note that contrary to naive expectations, an external magnetic field applied on the bath does not always reduce the rates as compared to the $H = 0$ case and in fact show a lot of anomalous behaviors. As $T \to 0$, both $\bar{\gamma}_1, \bar{\gamma}_2 \to 0$ for all H indicating non-Markovian behavior. At finite temperatures, as shown in the inset of Fig. 6, a common feature for the metallic and semiconducting baths is that both rates $\bar{\gamma}_1(H)$ and $\bar{\gamma}_2(H)$ have a non-monotonic dependence on H regardless of the value of the chemical potential μ. This non-monotonicity of the rates stems from the presence of a gap in the DOS since at high fields one is sensitive to the detailed nature of the DOS cf. Eq.(21). For example, such features are not seen in the case of a banal metallic bath described by $\rho(E) \propto \Theta(A - |E|)$.

At low temperatures, a straightforward calculation shows that for the semiconductor, $\bar{\gamma}_1^s(H) < \bar{\gamma}^s$ and for the metal, $\bar{\gamma}_1^m(H) < \bar{\gamma}^m$ if $H < \Delta$. Here $\bar{\gamma}^s$ and $\bar{\gamma}^m$ denote the corresponding $H = 0$ rates for the semiconducting and metallic baths discussed in the previous sections. On the other hand though $\bar{\gamma}_2^s(H) < \bar{\gamma}^s$ and $\bar{\gamma}_2^m(H) < \bar{\gamma}^m$ for $0 < H < |\Delta - \mu|$, if $|\Delta - \mu| < H < \Delta$ then $\bar{\gamma}_2^s(H) > \bar{\gamma}^s$ and $\bar{\gamma}_2^m(H) < \bar{\gamma}^m$. (see Table I). This difference between the metallic and semiconducting baths stems from the fact that for $H > |\Delta - \mu|$, changing the field is similar to changing the chemical potential (see eq. 21) and the bath switches from a metal-like behavior at low temperatures to a semiconductor-like behavior or viceversa. For extremely large fields $H \geq A$, the relaxation rate goes to zero as anticipated but the decoherence rate $\bar{\gamma}_2$ remains finite. This is true also for $h \neq 0$ but the critical field for which it happens is $H = A - h$. Note that in this high field limit an Ising like coupling would lead to both rates $\bar{\gamma}_{1,2} = 0$. The Markovian decoherence accompanied by zero rate of relaxation is a manifestation of the non-Ising nature of the coupling between the central spin and the bath. To summarize, fields $H < \Delta$ tend to partially suppress decoherence and relaxation induced by metallic baths. However, in the case of semiconducting baths, though fields $H < \Delta - \mu$ do partially suppress relaxation and decoherence, fields $|\Delta - \mu| < H < \Delta$ tend to augment decoherence.

B. $H = 0, h \neq 0$

In this case, where the central spin has intrinsic dynamics, Eq.(21) shows that $\bar{\gamma}_1 = \Gamma(\omega = 2h)$ and $\bar{\gamma}_2 = \Gamma(2h)/2 + \Gamma(0)/2$ (cf. Fig. 2). Consequently, both $\bar{\gamma}_1(h)$ and $\bar{\gamma}_2(h)$ have the same functional dependence on the central spin field h. We illustrate some scenarios where the intrinsic dynamics play an interesting role in Fig. 7. For a metallic bath, turning on a small field $0 < 2h < |\Delta - \mu|$ at $T = 0$ has the dramatic effect of transforming the non-Markovian decay of the decoherence and relaxation seen for $h = 0$ into a Markovian decay since $\bar{\gamma}_{1,2}^m \propto h$ for small h. At low temperatures (see Table I), for fields $0 < 2h < \Delta - \mu$, $\bar{\gamma}_{1,2}^m(h) > \bar{\gamma}^m$ whereas $\bar{\gamma}_{1,2}^s(h) < \bar{\gamma}^s$ due to the activation of the gap in Γ cf Fig. 2. Moreover, these rates increase monotonically with T and saturate to a finite value as $T \to \infty$.

The intermediate field regime yields the rather surprising result that for both metallic and semiconducting baths $\bar{\gamma}_1$ initially decreases with temperature, and then increases to attain a constant temperature independent value (blue curve Fig. 7). However, $\bar{\gamma}_2$ augments considerably in the same range of temperatures considered (red curve Fig. 7). Additionally, there exists a special value of the intrinsic field h_c for which the relaxation rate (blue curve Fig 7) has a reduced temperature dependence. This last feature also survives in the presence of a bath field H. For higher values of h, $\bar{\gamma}_1$ monotonically reduces with temperature but $\bar{\gamma}_2$ always increases with temperature (yellow and purple curves Fig 7). For all values of h, we have $\gamma_1 > \gamma_2$ for $T \lesssim \Delta$ and $\gamma_2 > \gamma_1$ for higher temperatures. To our knowledge, the possibility of an almost temperature independent relaxation at intermediate fields and the scenario where the relaxation rate decreases and the decoherence rate increases with temperature have not been discussed in the literature.

Interval/bath	Metallic	Semiconducting
$0 < H < \|\mu - \Delta\|, h = 0$	$\bar{\gamma}_{1,2}^m(H) < \bar{\gamma}_{1,2}^m$	$\bar{\gamma}_{1,2}^s(H) < \bar{\gamma}_{1,2}^s$
$\|\mu - \Delta\| < H < \Delta, h = 0$	$\bar{\gamma}_{1,2}^m(H) < \bar{\gamma}_{1,2}^m$	$\bar{\gamma}_1^s(H) < \bar{\gamma}_1^s$, $\bar{\gamma}_2^s(H) > \bar{\gamma}_2^s$
$0 < 2h < \|\mu - \Delta\|, H = 0$	$\bar{\gamma}_{1,2}^m(h) > \bar{\gamma}_{1,2}^m$	$\bar{\gamma}_{1,2}^s(h) < \bar{\gamma}_{1,2}^s$

TABLE I. Comparison between decoherence and relaxation rates $\bar{\gamma}_{1,2}^{m,s}(H,h)$ and $\bar{\gamma}_{1,2}^{m,s}$ for low temperatures and only one applied field.

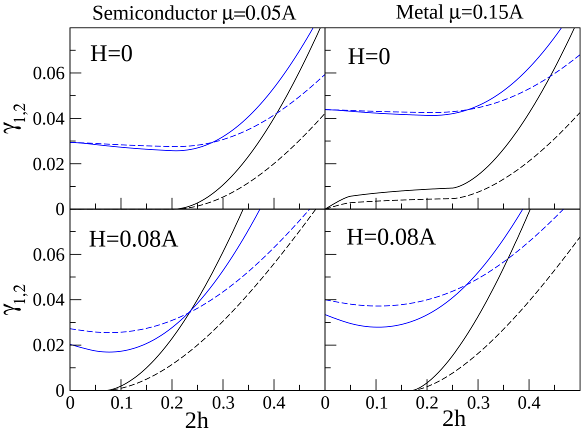

FIG. 8. (color online) Dimensionless relaxation (bold lines) and decoherence rate (dashed lines) $\gamma_{\bar{1},2}/N^2$ as functions of $2h$ for a semiconductor bath $\mu = 0.05A$ (left panel) and a metallic bath $\mu = 0.15A$ (right panel) for $T = 0$ (black) and $T = 0.1A$ (blue) for the elliptical DOS with $\Delta = 0.1A$ and $H = 0$ (top panel) and $H = 0.08A$ (bottom panel).

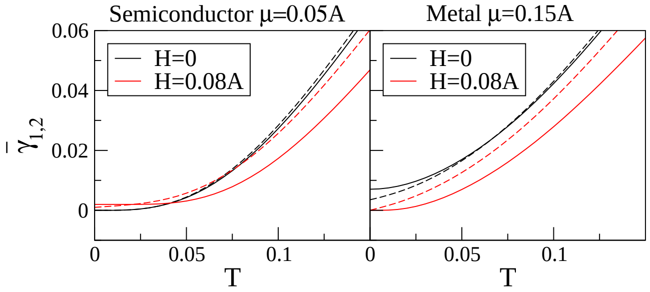

FIG. 9. (color online) Dimensionless relaxation (bold lines) and decoherence rate (dashed lines) $\bar{\gamma_{1,2}}/N^2$ as functions of T for a semiconductor bath $\mu = 0.05A$ (left panel) and a metallic bath $\mu = 0.15A$ (right panel) for $H = 0$ (black) and $H = 0.08A$ (red) for the elliptical DOS with $\Delta = 0.1A$ and $2h = 0.1A$.

C. $h \neq 0, H \neq 0$

In the presence of both fields, the low temperature behavior of the rates is an amalgam of the two cases studied above and is sensitive to the nature of the bath. The results for the relaxation rate $\bar{\gamma}_1(H, h)$ are plotted in Fig. 8 and Fig. 9 for both baths. For a given value of H and T, the decoherence and relaxation rates have the same functional dependence on h. We now consider the $T = 0$ case. Firstly, we note that at $T = 0$, $\bar{\gamma}_1(H, h) > \bar{\gamma}_2(H, h)$ for all reasonable fields irrespective of the nature of the bath. Moreover, for the metallic bath, if $0 < H < |\Delta - \mu|$ then both $\bar{\gamma}_{1,2}$ are non-zero for any finite field h. If the field is further increased $|\Delta - \mu| < H < \Delta + \mu$, then $\gamma_{1,2} = 0$ for $2h < \mu + \Delta - H$. This is clearly illustrated in the right panels of Fig. 8. As a result, the relaxation will be Markovian or non-Markovian depending on the values of h and H. The case of the semiconducting bath is the opposite: $\bar{\gamma}_{1,2}$ show a gap as a function of the field h for all $H \leq \Delta + \mu$, indicating non-Markovian behavior at low h and Markovian behavior for fields $2h > \Delta + \mu - H$ as shown in the left panels of Fig. 8. Finally, for large fields $H > \mu + \Delta$ any finite h leads to finite rates irrespective of the value of μ. Consequently, we have the surprising result that there exists a range of fields $max(\Delta + \mu_s - H, 0) < 2h < \Delta + \mu_m - H$ and $|\Delta - \mu_m| < H < \Delta + \mu_m$ where μ_s and μ_m denote the corresponding chemical potentials for the semiconducting and metallic baths, for which the metallic bath is more effective in suppressing relaxation and decoherence than the semiconducting bath. This feature persists at low temperatures $T \ll \Delta + \mu_s - H$, wherein there is a regime $h < h_1(T)$, where the semiconductor bath has lower rates as expected and a regime $h_1(T) < h < h_2(T)$, where the metallic bath has lower rates as compared to the semiconductor. The interval $h_2 - h_1 \to 0$ as temperature increases. In the first regime we find that $\bar{\gamma}_2 > \bar{\gamma}_1$ for all baths. We also see from Fig. 9 that for $0 < H, h < |\Delta - \mu|$ $\bar{\gamma}^s_1(H, h) < \bar{\gamma}^s_1(H) < \bar{\gamma}^s$ and $\bar{\gamma}^s_2(H, h) < \bar{\gamma}^s$. For larger fields $|\Delta - \mu| < H < \Delta$ and small enough h, $\bar{\gamma}^s_2(H, h) > \bar{\gamma}^s$ reminiscent of $h = 0$ case. For a metallic bath, if $0 < H < |\Delta - \mu|$ and $2h < \mu - \Delta - H$ then both the decoherence and the relaxation rate are greater than the decoherence and relaxation when no fields are present and we have $\bar{\gamma}^m_{1,2}(h) > \bar{\gamma}^m_{1,2}(H, h) > \bar{\gamma}^m$. At slightly higher temperatures, the semiconducting bath has a lower rate and at very high temperatures the two baths are indistinguishable as expected.

To summarize, we find that external magnetic fields do not necessarily reduce the relaxation and decoherence rates of the qubit. Depending on the nature of the bath and the values of the field, one sees a rich and varied behavior of the rates. For instance, in the absence of an intrinsic qubit field ($h = 0$), we find that the presence of a gap in the density of states leads to a non-monotonic variation of the rates as a function of the bath field H. In the presence of both fields, h and H, an interplay between the two magnetic fields leads to a very interesting regime wherein for a qubit field $h_1 < h < h_2$, the metallic bath has lower rates as compared to the semiconductor. The bounds h_1 and h_2 are functions of the gap Δ, the bath field H and the temperature. For any given H, there exists a value of the bath field h_c for which we have an almost temperature independent relaxation. For very high bath fields, the relaxation rate goes to zero but the decoherence rate remains finite signaling the non-Ising nature of the qubit-bath coupling. It would be very interesting to see if these features survive in the presence of an additional transverse field on the qubit.

V. DISCUSSION

We have studied the decoherence and relaxation of a central spin weakly coupled to a bath of electrons described by different densities of states having a gap, using two well known approximation schemes, NZ and TCL. Though both methods predict an asymptotic Markovian decay for a metallic bath, we have shown that in the case of a semiconducting bath, the TCL predicts a Markovian behavior at low T whereas the NZ approximation predicts non-Markovian behavior. The study of the validity of both approximation techniques is left for future work. We emphasize that one has to exert care when using approximation schemes to study the time evolution of the density matrix. We find that a gap in the spectrum, even one away from the Fermi level, generates an intermediate power law regime for the coherences at finite temperatures. Depending on the parameters of the problem, this power law regime can be made sufficiently large so as to be relevant for experiments. One might also question the validity of the weak coupling formalism used here since it is well known that even the equilibrium physics of the Kondo model is governed by strong coupling physics, which leads to a complete screening of the Kondo spin.

This was explored in Ref.[9], where numerical renormalization group methods were used to study the decoherence of the Kondo spin. It was found that for any value of the coupling λ there is a Kondo timescale $t_\lambda \propto \exp const/\lambda$ beyond which the Kondo spin gets screened dynamically. The weak coupling results discussed here were indeed valid for *intermediate* times $t \ll t_\lambda$. In this paper, since we are only interested in very small λ, we expect our results to be valid for realistically long times since the time scale $t_\lambda \to \infty$ as $\lambda \to 0$.

We have also calculated the relaxation and decoherence rate as a function of external magnetic fields applied on the bath and/or central spin. We encounter novel situations where for moderately large fields on the central spin alone result in a nearly temperature independent relaxation but a rapidly increasing decoherence. We find that the presence of gap anywhere in the density of states has important ramifications for the rates. This leads to the case where for a certain range of the bath field H, there is a regime $h_1(T) < h < h_2(T)$, where we have the surprising result that the metallic bath has lower rates of relaxation and decoherence as compared to the semiconductor. To conclude, there exists an interesting interplay between the gap in the density of states and the applied magnetic fields, which can have a lot of practical advantages for experiments on qubits.

-

Appendix A: Self-energy

Let us consider a general hamiltonian $H = H_S + H_B + H_{SB}$ where $H_S = -h\sigma_z$ and $H_{SB} = V_x\sigma_x + V_y\sigma_y + V_z\sigma_z$. The operators V are proportional to λ and λ is smaller than any other scale of the system. The Kondo coupling considered in this article is a specific case.

By following a procedure similar to the one presented in the appendix of[8] for the Ising coupling that uses the resolvent operator formalism[23] in the weak coupling regime one obtains the general form of the self energy matrix $\Sigma_{\beta\alpha}$ and $h_{\beta\alpha}$ in eq. (6). By definition $\Sigma_{0\alpha}(z) = 0$ for $\alpha = x, y, z$ and $\Sigma_{00}(z) = 1/z$ which assures the conservation of the trace. For the other components:

$$\Sigma_{\beta\alpha}(z) = -i\int_0^\infty dt e^{izt}\sum_{\gamma,\delta}(1-\delta_{\beta\gamma})\Big\{\langle\tilde{V}_\gamma(t)\tilde{V}_\delta\rangle \mathrm{Tr}\left(\sigma_c^\beta\sigma_c^\gamma e^{ith\sigma_c^z}\sigma_c^\delta\sigma_c^\alpha e^{-ith\sigma_c^z}\right) + \langle\tilde{V}_\delta\tilde{V}_\gamma(t)\rangle \mathrm{Tr}\left(\sigma_c^\gamma\sigma_c^\beta e^{ith\sigma_c^z}\sigma_c^\alpha\sigma_c^\delta e^{-ith\sigma_c^z}\right)\Big\} \tag{A1}$$

The $h_{\beta\alpha}$ are given by:

$$h_{\beta\alpha} = \frac{1}{2}\mathrm{Tr}\left(\sigma_\beta\left[H_S + \langle H_{SB}\rangle, \sigma_\alpha\right]\right) \tag{A2}$$

Where Tr it the total trace. For the specific case of the Kondo coupling:

$$h_{\beta\alpha} = \frac{1}{2}\mathrm{Tr}\left(\sigma_\beta\left[H_S, \sigma_\alpha\right]\right) \tag{A3}$$

since $\langle V_x\rangle = \langle V_y\rangle = \langle V_z\rangle = 0$ implying $\langle H_{SB}\rangle = 0$ for $H = 0$.

[1] M. A. Nielsen and I. L. Chuang, *Quantum Computation and Quantum Information.* (Cambridge University Press, 2000).

[2] S. Bose, Physical Review Letters **91**, 207901 (2003).

[3] Y. Makhlin, G. Schön, and A. Shnirman, Rev. Mod. Phys. **73**, 357 (2001).

[4] J. R. Petta, A. C. Johnson, C. M. Marcus, M. P. Hanson, and A. C. Gossard, Physical Review Letters **93**, 186802 (pages 4) (2004).

[5] A. O. Caldeira and A. J. Leggett, Phys. Rev. Lett. **46**, 211 (1981).

[6] A. J. Leggett, S. Chakravarty, A. T. Dorsey, M. P. A. Fisher, A. Garg, and W. Zwerger, Rev. Mod. Phys. **59**, 1 (1987).

[7] S. Camalet and R. Chitra, Phys. Rev. Lett. **99**, 267202 (2007).

[8] S. Camalet and R. Chitra, Phys. Rev. B **75**, 094434 (2007).

[9] F. B. Anders and A. Schiller, Phys. Rev. B **74**, 245113 (2006).

[10] P. C. E. Stamp and I. S. Tupitsyn, Phys. Rev. B **69**, 014401 (2004).

[11] D. Rossini, T. Calarco, V. Giovannetti, S. Montangero, and R. Fazio, Phys. Rev. A **75**, 032333 (2007).

[12] W. M. Witzel and S. Das Sarma, Phys. Rev. B **74**, 035322 (2006).

[13] N. Yamada, A. Sakuma, and H. Tsuchiura, J. Appl. Phys. **101** (2007), ISSN 0021-8979.

[14] Y. Gao and S.-J. Xiong, Physics Letters A **372**, 4630 (2008), ISSN 0375-9601.

[15] R. M. Lutchyn, L. Cywiński, C. P. Nave, and S. Das Sarma, Phys. Rev. B **78**, 024508 (2008).

[16] E. A. Winograd, M. J. Rozenberg, and R. Chitra, Phys. Rev. B **80**, 214429 (2009).

[17] H. P. Breuer and F. Petruccione, *The theory of Open Quantum Systems* (Oxford University Press, 2002).

[18] U. Weiss, *Quantum dissipative systems*, Series in modern condensed matter physics (World Scientific, 2008), ISBN 9789812791627.

[19] S. Dattagupta, H. Grabert, and R. Jung, Journal of Physics Condensed Matter **1**, 1405 (1989).

[20] H.-P. Breuer, D. Burgarth, and F. Petruccione, Phys. Rev. B **70**, 045323 (2004).

[21] A. Abragam, *The principles of nuclear magnetism*, International Series of Monographs on Physics (Oxford University Press, 1994), ISBN 9780198520146.

[22] C. Kittel, *Introduction to Solid State Physics* (Wiley, New York, 1971), 4th ed., ISBN 0-471-49021-0.

[23] G. G. Claude Cohen-Tannoudji, Jacques Dupont-Roc, *Atom-Photon Interactions: Basic Processes and Applications* (1998).